Biomatemática ***34*** *(2024), 15–44* ***ISSN 1679-365X***
A publication of Biomathematics group IMECC – Unicamp

State feedback as a strategy for COVID-19 control and analysis

Leonardo R. S. Rodrigues[1], Felipe Gabrielli[2]
Natural Sciences, CCCO, UFMA – 65.400-000, Codó/MA.

Abstract. This paper presents a study on a compartmental epidemic model for COVID-19, examining the stability of its equilibrium points upon vaccination introduction as a strategy to mitigate the spread of the disease. Initially, the Susceptible-Infectious-Quarantine-Recovered (SIQR) mathematical model and its technical aspects are introduced. Subsequently, vaccination is incorporated as a control measure within the model scope. Equilibrium points and the basic reproductive number are determined followed by an analysis of their stability. Furthermore, controllability characteristics and optimal control strategies for the system are investigated, supplemented by numerical simulations.

Keywords*: Optimal, mathematical modeling, Riccati, equilibrium points, vaccination, numerical simulation.*

1. Introdution

Mathematical modeling has long been used as a tool in several areas of public health, including epidemiology, an area that developed significantly during the 20^{th} century. Models in mathematical epidemiology, in particular, have been studied since the 18^{th} century but had a development leap arguable from the work of Kermark and Mckendrick (1927). Since then, many other advances were made and many types of models were created and studied. Most of these models are compartmental models, which divide the population into categories with a particular behavior. Some examples are SIS, SIR, SIRS, SEIR,

[1]leonardo.rodrigues@ufma.br
[2]gabrielli14@gmail.com

SIQR, among others. More details about some of these models can be seen in Brauer et al. (2019). One important point to observe is that a mathematical model is always a simplification of reality. Some aspects are disregarded, so we can focus on the variables that really matter to the problem. No model can consider all aspects of a complex real problem, as the spread of an infectious disease, hence the importance of each model type. Just to exemplify this reality simplification, the model studied in this paper does not consider population heterogeneity, i.e, all individuals are equally susceptible to the disease, and there are models that take these differences into account, as can be seen in Britton et al. (2020).

We are currently living through the COVID-19 pandemic, a disease caused by the sars-cov-2 virus, which has already caused thousands of deaths around the world and continues to plague the population. Many researchers believe that COVID-19 will become an endemic disease in the future, but until the present date, World Health Organization keeps classifying COVID-19's threat level as a pandemic. An interesting discussion about predicting the pandemic contention is done by Achaiah et al. (2020). Several strategies have been adopted by governments to combat the spread of the disease, such as quarantine, lockdown, closing borders, using masks, hand hygiene with alcohol gel, etc. But no measure is as effective as vaccination, and since its development in 2021, many countries have implemented a vaccination schedule as part of disease-fighting strategies. Vaccination is the most effective and safe way we know to combat infectious diseases, and it was responsible, for instance, for eradicating smallpox.

Our objective in this work is to consider and analyze the SIQR model properties by adding vaccination as a strategy to control the growth of the disease, study constant solution stability, calculate the basic reproductive number of disease propagation, study system controllability and the conditions to obtain the optimal control and apply the model in some numerical simulations (using MATLAB^{TM} software) to reach some conclusions about the control method (vaccination).

This analysis, via theoretical modeling, is very important to complement the models that work with empirical data to compare, complement and adjust possible strategies to face the disease, given that empirical data is not entirely trustful, as can be seen in Liu et al. (2020), due to the number of unreported cases and the low number of tests in many countries.

2. SIQR mathematical model

In this section, we will describe the mathematical model used to study the spreading of COVID-19, its elements, and technical features.

In order to study the spread of infectious disease, we have to consider a population whose size varies with time, representing this population as $N(t)$ – see equation (2.1). The mathematical model we will use is a SIQR compartmental model that divides the total population into four groups, such as susceptible ($S(t)$), infected ($I(t)$), quarantined ($Q(t)$) and recovered (sometimes also called removed) ($R(t)$), thus:

$$N(t) = S(t) + I(t) + Q(t) + R(t) \tag{2.1}$$

The model is the following system (2.2) of ordinary differential equations:

$$\begin{cases} \frac{dS}{dt} = \Delta - \alpha SI - \mu S \\ \frac{dI}{dt} = \alpha SI - (\gamma + \mu + \eta)I \\ \frac{dQ}{dt} = (\eta - \epsilon)I - (\rho + \mu)Q \\ \frac{dR}{dt} = \gamma I + \rho Q - \mu R \end{cases} \tag{2.2}$$

Such as:

Table 1: Model parameters

Variable	**definition**
T	Time
α	Effective contact rate between susceptible and infectious class
γ	Natural recovery rate
μ	Natural death rate
ρ	Removed rate from quarantine to recovered
ϵ	Disease-related death rate
η	Infectious class quarantine rate
Δ	Population recruitment rate

The model works with the following dynamics:each compartment has an initial portion proportional to the population N, and if we want to encourage the start of the pandemic, for example, we can put $Q(0) = 0$, $R(0) = 0$ and even $I(0) = I/N$ (representing patient zero). After that, the parameters will change the population amounts in each compartment at each time interva, adding or

subtracting some portions. In the first equation, the susceptible population is increased by Δ, then some portion (determined by α) is subtracted from the susceptible and added to the infectious group. Still in the first equation, another portion is subtracted due to μ, the natural death rate. The population in the second group is also decreased by μ and by γ and η, natural recovery rate and quarantine rate, respectively. The third and fourth equations follow the same dynamics. In the third, a portion (due to ϵ) is subtracted, representing the disease-related death rate, and another portion is subtracted from there and added to the recovered group (ρ), representing the quarantine recovery rate.

Figure 1 shows a schematic diagram showing the model dynamics:

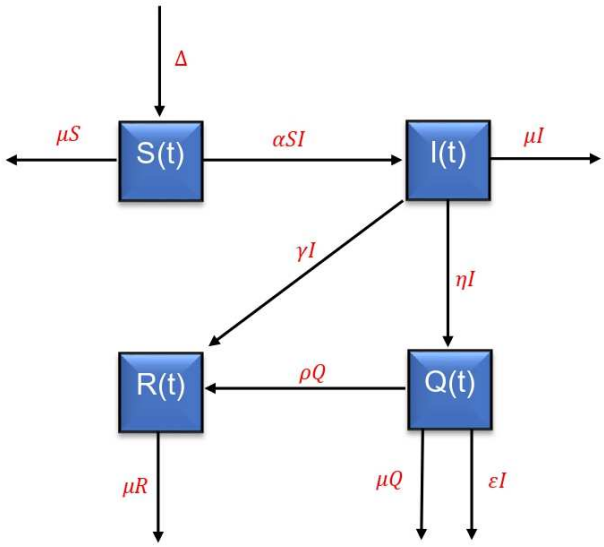

Figure 1: SIQR dynamic flow

Some important observations about this model are

- As already mentioned, this is a homogeneous-mixing model;
- It uses only one disease-related death rate (some models have different death-related rates for infected and quarantine individuals, such as Lisboa and Rodrigues (2023));

– This model does not consider an incubation period;

– It does not differentiate infected individuals with symptoms and without symptoms. They are all in the same group;

– In the quarantine compartment, isolated individuals are those who are infected, and it does not consider the isolation of healthy individuals.

More details about the SIQR model properties can be found in Lu et al. (2021), Ma et al. (2018) and Odagaki (2020). Lisboa and Rodrigues (2023) they use a slightly different SIQR model and even make simulations based on empirical data from local healthcare authorities.

Now we complete our model by adding vaccination as a control agent for the system:

$$\begin{cases} \frac{dS}{dt} = \Delta - \alpha SI - \mu S - vS \\ \frac{dI}{dt} = \alpha SI - (\gamma + \mu + \eta)I \\ \frac{dQ}{dt} = (\eta - \epsilon)I - (\rho + \mu)Q \\ \frac{dR}{dt} = \gamma I + \rho Q - \mu R \end{cases} \tag{2.3}$$

In system (2.3) the v parameter represents the presence of vaccination, and the portion of the population who are vaccinated is subtracted from the susceptible group and added directly to the recovered group. It is easy to observe that the higher the percentage of vaccinated individuals, the lower the proportion of infected individuals and, consequently, the lower the number of disease-related death. We now proceed to a qualitative analysis of the system of differential equations, presented in (2.3).

3. Methodology

To study and analyze disease-free equilibrium and endemic equilibrium point stability, we used the Routh-Hurwitz criteria, Lyapunov method and La Salle's invariance principle.

To study and analyze control system controllability, we used Kalman criteria, studies the control problem with linear dynamics and quadratic objective function and used a Riccati equation to obtain the corresponding optimal controls. To solve the problems, we used the fourth order Runge-Kutta method, and in numerical simulations, we used MATLAB^{TM} software.

4. Equilibrium points and basic reproductive number

In this section, we found the constant solutions (equilibrium points) of system (2.3) and showed the formula for the basic reproductive number.

We will call R_0 the basic reproductive number of a disease, which indicates how contagious an infectious disease is. This number is very important to healthcare authorities and governments to devise strategies to combat the disease. To learn more about R_0, one can look at Achaiah et al. (2020) and Ma (2020).

Theorem 4.1. *The closed region* $\Omega = \left\{(S, I, Q, R) \in \mathbb{R}^4_+ : N(t) \leq \frac{\Delta}{\mu}\right\}$ *is positive invariant ste for the model (2.3).*

Proof. To initiate our analysis, we have to establish boundaries to our variables and parameters. All parameters described in table 1 are non-negative real numbers. For our variables, we used the derivative of $N(t)$ in expression (2.1):

$$N'(t) = \Delta - \mu N - \epsilon I \leq \Delta - \mu N$$

Multipling by integration factor $e^{\mu t}$:

$$N'(t)e^{\mu t} \leq \Delta e^{\mu t} - \mu N e^{\mu t}$$

$$N'(t)e^{\mu t} \leq \Delta e^{\mu t} - \mu N e^{\mu t}$$

Integrating both sides:

$$\int_o^t [N'(t)e^{\mu t} + \mu N e^{\mu t}]\, dt \leq \int_o^t \Delta e^{\mu t}\, dt$$

$$N(t)e^{\mu t}\Big|_0^t \leq \Delta \frac{e^{\mu t} - 1}{\mu}\Big|_0^t$$

$$e^{\mu t}N(t) - N(0) \leq \Delta\left(\frac{e^{\mu t} - 1}{\mu}\right)$$

$$N(t) \leq N(0)e^{-\mu t} + \frac{\Delta}{\mu}(1 - e^{-\mu t})$$

When $x \to \infty$, we have:

$$\lim_{x\to\infty} Sup[N(t)] = \frac{\Delta}{\mu}$$

This shows us that we have to study the problem in region D:

$$D = \left\{ (S, I, Q, R) | S \geq 0, I \geq 0, Q \geq 0, R \geq 0, S + I + Q + R \leq \frac{\Delta}{\mu} \right\}$$

□

4.1. Positivity and boundedness

Theorem 4.2. *Let $(S(0), I(0), Q(0), R(0))$ be non negative initial conditions, then the solutions $(S(t), I(t), Q(t), R(t))$ of the proposed model* (2.3) *are positive for all $t > 0$.*

Proof. Consider the following from the model's first equation (2.3)

$$\begin{aligned} \frac{dS}{dt} &= \Delta - \alpha SI - \mu S - vS \\ \frac{dS}{dt} &\geq -(\alpha I + \mu + v)S \\ S(t) &\geq Ce^{-(\alpha I + \mu + v)t} \end{aligned}$$

where $C = e^{C_1}$ is a constant determined by the initial conditions. Now, if $S(0)$ is the initial condition, then $S(0) = C$, so we can state that:

$$S(t) \geq S(0)e^{-(\alpha I + \mu + v)t}$$

Therefore, the solution $S(t)$ is bounded above by $S(0)$.
By using the same justification, we can demonstrate that:

$$Q(t) \geq Q(0)e^{-(\rho + \mu)t}$$

and

$$R(t) \geq R(0)e^{-\mu t}, \text{ for all } t > 0.$$

We have proved the lemma technical by showing that $I(t)$ is bounded. In fact:

Lemma 4.3. *Let the solution $S(t)$ be bounded below by $S(0)e^{-(\alpha I(t) + \mu + v)t}$ for all $t > 0$, where $S(0)$ is the initial condition. Then, the solution $I(t)$ of the differential equation*

$$\frac{dI}{dt} = \alpha SI - (\gamma + \mu + \eta)I$$

is bounded for all $t > 0$.

Proof. We are given the constraint that $S(t) \geq S(0)e^{-(\alpha I(t)+\mu+v)t}$. This constraint means that the $S(t)$ value will never decrease below $S(0)e^{-(\alpha I(t)+\mu+v)t}$. Under this condition, any increase in $I(t)$ that would cause $S(t)$ to decrease below the specified limit contradicts the imposed constraint on the $S(t)$ dynamics. This is a direct consequence of the interdependence between $S(t)$ and $I(t)$, as described by equations (2.3). Therefore, the solution $I(t)$ is bounded, ensuring that $S(t)$ remains above the specified limit for all $t > 0$. □

This demonstrates that the soluton of system (2.3) is positive for all $t > 0$. As a result, the model is epidemiologically significant and mathematically placed in the Ω domain. □

By setting the right side of system (2.3) to zero, we have:

$$\begin{cases} \Delta - \alpha SI - \mu S - vS = 0 \\ \alpha SI - (\gamma + \mu + \eta)I = 0 \\ (\eta - \epsilon)I - (\rho + \mu)Q = 0 \\ \gamma I + \rho Q - \mu R = 0 \end{cases} . \tag{4.4}$$

We established the existence of a disease-free constant solution and an endemic constant solution:

Theorem 4.4. *For system (4.4), there is always a disease-free equilibrium E_0, and there is also an unique endemic equilibrium E^*.*

Proof. By observing the second equation in system (4.4), we have the product:

$$I[\alpha S - (\gamma + \mu + \eta)] = 0 \tag{4.5}$$

If we have $I = 0 \Rightarrow Q = 0$, $S = \frac{\Delta}{\mu+v}$ and $R = 0$

Thus, the point $E_0 = \left(\frac{\Delta}{\mu+v}, 0, 0, 0\right)$ is a solution called free-disease solution.

If $[\alpha S - (\gamma + \mu + \eta)] = 0$, then:

$$S^* = \frac{\gamma + \mu + \eta}{\alpha}$$

By replacing S^* in the first equation of (4.4), we have:

$$\Delta - (\gamma + \mu + \eta)\left(I^* + \frac{\mu + v}{\alpha}\right) = 0$$

$$I^* = \frac{\Delta}{\gamma+\mu+\eta} - \frac{\mu+v}{\alpha}$$

$$I^* = \frac{\mu+v}{\alpha}\left(\frac{\Delta}{\mu+v}\frac{\alpha}{\gamma+\mu+\eta} - 1\right)$$

By proceeding in the same way in the third and fourth equations, we have:

$$Q^* = \frac{(\eta-\epsilon)I^*}{\rho+\mu}$$

$$R^* = \frac{\gamma I^* + \rho Q^*}{\mu}$$

$E^* = (S^*, I^*, Q^*, R^*)$ is called endemic solution. □

By looking at expression of I^*, it is important to note that equilibrium point E^* only occurs if:

$$\left(\frac{\Delta}{\mu+v}\frac{\alpha}{\gamma+\mu+\eta} - 1\right) > 1$$

Thus, we defined:

Definition 4.5. The basic reproduction number for system (2.3), denoted by R_0, is given as:

$$R_0 = \left(\frac{\Delta}{\mu+v}\frac{\alpha}{\gamma+\mu+\eta}\right). \tag{4.6}$$

which represents the mean number of new infections generated by an infectious case in a susceptible population.

Expression (4.6) is essential to system (2.3). If $R_0 > 1$, then the solution converge to the endemic equilibrium. On the other hand, if $R_0 < 1$, then the solution converge to free-disease equilibrium.

The R_0 value for COVID-19 is estimated to be between 1.9 and 6.5 according to Achaiah et al. (2020).

5. Equilibrium point stability

In this section, we will state and prove the theorems that establish the stability of the solutions found in the previous section.

Theorem 5.1. *If $R_0 < 1$, disease-free equilibrium E_0 of system (2.3) is locally asymptotically stable. If $R_0 > 1$, the disease-free equilibrium E_0 is unstable.*

Proof. The Jacobian matrix of system (2.3) at E_0 is:

$$J(E_0) = \begin{bmatrix} -\mu - v & -\frac{\alpha\Delta}{\mu+v} & 0 & 0 \\ 0 & \frac{\alpha\Delta}{\mu+v} - (\gamma+\mu+\eta) & 0 & 0 \\ 0 & (\eta-\epsilon) & -(\rho+\mu) & 0 \\ 0 & \gamma & \rho & -\mu \end{bmatrix}$$

The four eigenvalues of matrix $J(E_0)$ are:

$$\lambda_1 = -\mu - v, \lambda_2 = \frac{\alpha}{\gamma+\mu+\eta}(R_0 - 1), \lambda_3 = -(\rho+\mu), \lambda_4 = -\mu$$

If $R_0 < 1 \Rightarrow \lambda_2 < 0$, therefore, all eigenvalues have negative real parts and E_0 is locally asymptotically stable. If $R_0 > 1 \Rightarrow \lambda_2 > 0$, thus E_0 is unstable. □

Theorem 5.2. *If $R_0 < 1$, the disease-free equilibrium E_0 of the system* (2.3) *is globally asymptotically stable.*

Proof. Consider the following Lyapunov function:

$$\mathcal{L}(t) = I(t)$$

By calculating the derivative of $\mathcal{L}(t)$ along the positive solution of system (2.3), we have that:

$$\begin{aligned} \left.\frac{d\mathcal{L}(t)}{dt}\right|_{(3)} &= \left.\frac{dI}{dt}\right|_{(3)} = \alpha SI - (\gamma+\mu+\eta)I \\ &= [\alpha S - (\gamma+\mu+\eta)]I \\ &= \left[\alpha\frac{\Delta}{\mu+v} - (\gamma+\mu+\eta)\right]I \\ &= [(\gamma+\mu+\eta)(R_0-1)]I \\ &\leq 0 \end{aligned}$$

Furthermore, $\mathcal{L}' = 0$ only if $I = 0$. The maximum invariant set in $\{(S, I, Q, R)|\mathcal{L}' = 0\}$ is the singleton E_0. When $R_0 < 1$, according to La Salle's invariance principle, we have that:

$$\lim_{t\to\infty} I(t) = 0$$

Then, we obtain the limit equations of system (2.3):

$$\begin{cases} \frac{dS}{dt} = \Delta - \mu S - vS \\ \frac{dQ}{dt} = -(\rho + \mu)Q \\ \frac{dR}{dt} = \rho Q - \mu R \end{cases} .$$

Thus, disease-free equilibrium is globally attractive in region D. Therefore, disease-free equilibrium of system (2.3) is globally asymptotically stable when $R_0 < 0$. □

Theorem 5.3. *If $R_0 > 1$, endemic equilibrium E^* of system (2.3) is locally asymptotically stable.*

Proof. The Jacobian matrix of system (2.3) at E^* is:

$$J(E^*) = \begin{bmatrix} -\alpha I^* - \mu - v & -\alpha S^* & 0 & 0 \\ \alpha S^* & 0 & 0 & 0 \\ 0 & (\eta - \epsilon) & -(\rho + \mu) & 0 \\ 0 & \gamma & \rho & -\mu \end{bmatrix}$$

The two eigenvalues of matrix $J(E^*)$ are:

$$\lambda_3 = -(\rho + \mu), \lambda_4 = -\mu$$

The other two eigenvalues are also the eigenvalues of the following matrix:

$$J^*(E^*) = \begin{bmatrix} -(\alpha I^* + \mu + v) & -\alpha S^* \\ \alpha S^* & 0 \end{bmatrix}$$

which has the characteristic polynomial:

$$\lambda^2 + (\alpha I^* + \mu + v)\lambda + \alpha^2 {S^*}^2 = 0$$

which has all coefficients positive. By applying the Routh-Hurwitz criterion, we obtained that all eigenvalues of matrix $J(E^*)$ have negative real parts and endemic equilibrium E^* is locally asymptotically stable. □

Theorem 5.4. *If $R_0 > 1$, endemic equilibrium E^* of system (2.3) is globally asymptotically stable.*

Proof. If $R_0 > 1$ we have that endemic equilibrium point values are given by

$$E^* = \left(\frac{\gamma + \mu + \eta}{\alpha}, \frac{\mu + v}{\alpha}(R_0 - 1), \frac{(\eta - \epsilon)I^*}{\rho + \mu}, \frac{\gamma I^* + \rho Q^*}{\mu} \right).$$

Consider the following Liapunov function:

$$\mathcal{L}(t) = \frac{1}{2}\left[(S - S^*) + (I - I^*) + (Q - Q^*) + (R - R^*)\right]^2.$$

By calculating the derivative of $\mathcal{L}(t)$ with respect to t, we have that

$$\frac{d\mathcal{L}}{dt} = \left[(S - S^*) + (I - I^*) + (Q - Q^*) + (R - R^*)\right] \frac{d}{dt}\left[S + I + Q + R\right],$$

since $N(t) = S + I + Q + R$, and according to Theorem 4.1, we have $N'(t) \leq (\Delta - \mu N)$ and consequently $N(t) \leq \dfrac{\Delta}{\mu}$. So,

$$\begin{aligned} \frac{d\mathcal{L}}{dt} &= \left[(S - S^*) + (I - I^*) + (Q - Q^*) + (R - R^*)\right] \frac{dN}{dt} \\ &\leq \left[(S - S^*) + (I - I^*) + (Q - Q^*) + (R - R^*)\right] (\Delta - \mu N) \\ &\leq (N - \frac{\Delta}{\mu})(\Delta - \mu N) \end{aligned}$$

Finally, we have:

$$\frac{d\mathcal{L}}{dt} \leq -\frac{1}{\mu}(\Delta - \mu N)^2.$$

We can clearly determine that $\mathcal{L}'(t)$ is negative definite and $\mathcal{L}(t)$ is positive definite. Furthermore, $\frac{d\mathcal{L}}{dt} = 0$ if and only if $S = S^*, I = I^*, Q = Q^*, R = R^*$. Therefore, the largest compact invariant set of $\{\mathcal{L}'(t) = 0\}$ is the singleton E^*. This shows that, according to the classical Lyapunov and La Salle's invariance principle, E^* is globally asymptotically stable. Thus, system (2.3) has a globally asymptotically stable solution (S^*, I^*, Q^*, R^*). □

6. Finite dimensional linear system control

Let $T > 0$ be a real fixed number. We should consider the following finite dimensional system:

$$\begin{aligned} x'(t) &= Ax(t) + Bu(t),\ t \in [0, T] \\ x(0) &= x_0, \end{aligned} \tag{6.7}$$

where $A \in \mathbb{R}^{n,n}$, $B \in \mathbb{R}^{n,m}$ are a real matrix, and x_0 is a vector in $\mathbb{R}^n$. The function $x : [0,T] \to \mathbb{R}^n$ represents the state, and $u : [0,T] \to \mathbb{R}^m$, the control. Both are vector functions of m and n components, respectively, depending exclusively on time t.
Given an initial datum $x_0 \in \mathbb{R}^n$ and a vector function $u \in L^1([0,T];\mathbb{R}^m)$, system (6.7) has a unique solution $C([0,T];\mathbb{R}^n)$ characterized by the variation of constants formula:

$$x(t) = e^{At}x_0 + \int_0^t e^{A(t-s)}Bu(s)ds, \ \forall t \in [0,T].$$

6.1. Kalman's controllability rank condition

The following classical result is due to Micu and Zuazua (2004) and gives a complete answer to the problem of exact controllability of finite dimensional linear systems. It shows, in particular, that the control time is irrelevant.

We considered that $A \in \mathbb{R}^{4,4}$ is the Jacobian matrix of system (2.2) at E_0 without coontrol perturbation; $B \in \mathbb{R}^{4,2}$ is a real matrix; and x_0 is a vector in $\mathbb{R}^4$. The function $x : [0,T] \to \mathbb{R}^4$ represents the state, and $u : [0,T] \to \mathbb{R}^2$, the control. Both are vector functions of 4 and 2 components, respectively, depending exclusively on time t. We will use the shorthand notation (A,B) to denote control system (6.7).

Definition 6.1. A system (A,B), for which the Kalman criterion condition is satisfied, is termed completely controllable.

Theorem 6.2. *System* (6.7) *is completely controllable in some time T if and only if*

$$rank[B, AB, A^2B, A^3B] = 4.$$

Consequently, if system (6.7) *is controllable in some time $T > 0$, it is controllable in any time.*

Proof. In fact, from (6.7), we have

$$A = \begin{bmatrix} -\mu & 0 & 0 & 0 \\ 0 & -(\gamma+\mu+\eta) & 0 & 0 \\ 0 & (\eta-\epsilon) & -(\rho+\mu) & 0 \\ 0 & \gamma & \rho & -\mu \end{bmatrix}$$

and

$$B = \begin{bmatrix} 1 & 0 \\ 0 & 1 \\ 0 & 0 \\ 0 & 0 \end{bmatrix}.$$

with μ, γ, η, ϵ and ρ being positive constants. To determine system controllability, we calculated the controllability matrix $W_c = [B, AB, A^2B, A^3B]$. Consequently, we have

$$rank\ W_c = 4.$$

Therefore, the system is controllable.

In conclusion, **Algorithm 1** shows the matrix calculation.

Algorithm 1. Solving the matrix W_c

1: **Constant values**
2: mu = 0.02;
3: alpha = 0.2;
4: Delta = 0.2;
5: gamma = 0.1;
6: eta = 0.2;
7: epsilon = 0.1;
8: rho = 0.3;
9: **Definition of matrix A**
10: A = [-mu , 0, 0, 0; 0, -(gamma + mu + eta), 0, 0;
11: 0, eta - epsilon, -(rho + mu), 0;
12: 0, gamma, rho, -mu];
13: **Definition of matrix B**
14: B = [1 0;0 1;0 0;0 0];
15: **Controllability check**
16: $Wc = [B, AB, A^2B, A^3B]$;
17: $rank_W c = rank(Wc)$;
18: **Show the position of the W_c matrix**
19: $disp([' Posto\ da\ matriz\ Wc:\ ' num2str(rank_W c)])$

□

Figure 2 shows, that the number of columns in Matrix W_c equals the order of the system, indicating complete controllability. However, columns 1

and 2 exhibit singular values significantly different from zero, suggesting their importance in system controllability. Thus, the presence of these significant singular values implies that columns 1 and 2 of the controllability matrix are crucial for system controllability.

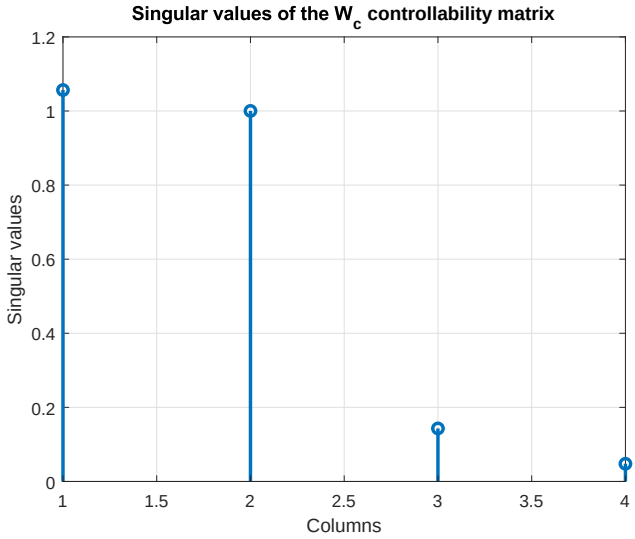

Figure 2: Controllability matrix

In the context of working with an epidemiological model that provides insights into the spread of COVID-19, it is highly advantageous to employ output feedback and State Feedback Strategies to modify the free system dynamics, aiming to achieve properties such as full controllability, asymptotic stability, BIBO-stability, etc. At this stage of the research, we are interested in demonstrating that, in the case of autonomous linear control system, given $A \in \mathbb{R}^{n,n}$ and $B \in \mathbb{B}^{n,m}$, we have:

$$x' = Ax + Bu. \tag{6.8}$$

We can utilize the state feedback strategy, where we assume that the control u is derived from the state x through a linear law, denoted as

$$u = -Fx, \tag{6.9}$$

where $F \in \mathbb{R}^{m,n}$ is a state feedback *Gain Matrix*. By replacing them (6.8), we

obtained:

$$x' = (A + BF)x.$$

The subsequent outcome facilitates our examination of controllability concerns in the presence of disturbances within a completely controllable autonomous system.

Theorem 6.3. *Let (A, B) be a completely controllable autonomous system. Then, for every matrix $F \in \mathbb{R}^{2,4}$, system $(A + BF, B)$ is also completely controllable.*

Proof. Note that

$$A = \begin{bmatrix} -\mu & 0 & 0 & 0 \\ 0 & 0 - (\gamma + \mu + \eta) & 0 & 0 \\ 0 & (\eta - \epsilon) & -(\rho + \mu) & 0 \\ 0 & \gamma & \rho & -\mu \end{bmatrix}$$

and

$$B = \begin{bmatrix} 1 & 0 \\ 0 & 1 \\ 0 & 0 \\ 0 & 0 \end{bmatrix}.$$

Given

$$F = -\begin{bmatrix} v & \frac{\alpha\Delta}{\mu+v} & 0 & 0 \\ 0 & -\frac{\alpha\Delta}{\mu+v} & 0 & 0 \end{bmatrix}$$

by (6.9) assuming that the control u is

$$u = -\begin{bmatrix} v & \frac{\alpha\Delta}{\mu+v} & 0 & 0 \\ 0 & -\frac{\alpha\Delta}{\mu+v} & 0 & 0 \end{bmatrix} \begin{bmatrix} S \\ I \\ Q \\ R \end{bmatrix},$$

that result in

$$u = \begin{bmatrix} -vS - \frac{\alpha\Delta}{\mu+v} I \\ \frac{\alpha\Delta}{\mu+v} I \end{bmatrix}.$$

Consequently, we obtain

$$(A + BF) = \begin{bmatrix} -\mu - v & -\frac{\alpha\Delta}{\mu+v} & 0 & 0 \\ 0 & \frac{\alpha\Delta}{\mu+v} - (\gamma + \mu + \eta) & 0 & 0 \\ 0 & (\eta - \epsilon) & -(\rho + \mu) & 0 \\ 0 & \gamma & \rho & -\mu \end{bmatrix},$$

noting that $(A + BF)$ is the Jacobian matrix of system (2.3) at point E_0 with the presence of control perturbation. To prove the given theorem, we will use the Kalman criterion for linear system controllability.

The Kalman criterion states that a linear system is completely controllable if its controllability matrix:

$$\mathcal{C} = [B \quad AB \quad A^2B \quad A^3B]$$

And has full rank, meaning its rank equals state-space dimension.

Now, we will use the Kalman criterion to prove the given theorem. Given a system (A, B) that is completely controllable, we know that the controllability matrix $\mathcal{C}$ has full rank, which means the rank of $\mathcal{C}$ equals state-space dimension.

The dimension state-space dimension equals 4. Then, the rank of $\mathcal{C}$ is 4. Now, considering system $(A + BF, B)$, F is a control matrix.

The controllability matrix of this system is:

$$\mathcal{C}_{\text{new}} = [B \quad (A + BF)B \quad (A + BF)^2B \quad (A + BF)^3B]$$

Now, we need to show that the rank of $\mathcal{C}_{\text{new}}$ equals to 4, i.e., full rank. If we can show this, then system $(A + BF, B)$ will be completely controllable. To do this, we will use the property that the rank of a matrix does not change when we multiply the matrix by another left-invertible matrix. We will use this property to show that the rank of $\mathcal{C}_{\text{new}}$ equals 4.

We will consider the matrix T defined as:

$$T = \begin{bmatrix} I & 0 & 0 & 0 \\ F & I & 0 & 0 \\ F^2 & 2BF & I & 0 \\ F^3 & 3BF^2 & 3B(F^2 + BF + I) & I \end{bmatrix}$$

where I is the identity matrix. It is easy to see that T is an invertible matrix.

Furthermore, if we multiply T by the matrix $\mathcal{C}_{\text{new}}$, we obtain $\mathcal{C}$.

$$T\mathcal{C}_{\text{new}} = [B \quad AB \quad A^2B \quad A^3B] = \mathcal{C}$$

Since $\mathcal{C}$ has full rank (equal to n), then $T\mathcal{C}_{\text{new}}$ also has full rank.

Therefore, the rank of $\mathcal{C}_{\text{new}}$ equals 4, and thus system $(A + BF, B)$ is completely controllable.

Thus, using the Kalman criterion, we have proven that, for every matrix F, system $(A + BF, B)$ is completely controllable, provided that (A, B) is

completely controllable. In conclusion, **Algorithm 1** shows the calculation of the matrix $(A + BF)$ with the appropriate changes to the input values. This concludes the proof of the theorem. □

7. Optimal control model

In this section, we associated the control problem (2.3) with a function that is intrinsically related to solving the system problem. This relationship is described through the optimality principle of a dynamic system. We wanted to find a control function that minimizes or maximizes a cost functional while satisfying the constraints imposed by the system. Thus, the following optimal control variable is given: the variable $u(t)$ represents vaccination, as seen previously. In this context, optimal control theory provides a powerful framework for designing control strategies that minimize the spread of infectious diseases while considering various constraints and objectives. By formulating the problem as an optimization task, optimal control theory allows us to determine the most effective allocation of control measures over time to achieve specific objectives, such as minimizing the number of infections, reducing economic losses, or optimizing the use of healthcare resources.

We treated a special case in optimal system control, in which state differential equations are linear in x and u and the objective functional is quadratic.

Let $T > 0$ be a fixed real number, given $t_0 \in [0, T]$ and $x_0 \in \mathbb{R}^n$, considering a dynamic system described by the following differential equations:

$$\begin{aligned} x'(t) &= Ax(t) + Bu(t),\ t \in [0, T] \\ x(t_0) &= x_0, \end{aligned} \tag{7.10}$$

considering cost functional

$$J(u, x) = \frac{1}{2}\left[\int_0^T x^{\mathbf{T}}(t)G(t)x(t) + u^{\mathbf{T}}(t)R(t)u(t)dt\right] \tag{7.11}$$

in which the matrices $G(t)$ and $R(t)$ are sizes $n \times n$, $m \times m$, respectively, with $G(t)$ being positive semidefinite and $R(t)$ being positive definite for all $t \in [0, T]$. The positive definite property guarantees that $R(t)$ is invertible. The superscript $\mathbf{T}$ refers to transpose of a matrix.

Considering the set of admissible control

$$\mathcal{U}_{ad} := \left\{u \in L^1([0, T]; \mathbb{R}^m); u(t) \in \mathcal{X} \subset \mathbb{R}^m \ a.e\ in\ [t_0, T].\right\}$$

Definition 7.1. The optimal value function refers to the application $V : [0,T] \times \mathbb{R}^n \to \mathbb{R}$, defined by

$$V(t_0, x_0) := inf \left\{ J(t_0, x_0; u);\ u \in \mathcal{U}_{ad} \right\}.$$

Definition 7.2. The optimal control problem is to find, for a given initial condition x_0, the control $u^* \in \mathcal{U}_{ad}$ that minimizes the cost functional (7.11). Furthermore,

$$V(t_0, x_0) = J(t_0, x_0; u^*).$$

With the objective of illustrating the ideas presented here, we considered the control problem (7.10) to (7.11). The Hamiltonian becomes

$$H(t, x, u, \lambda) := \frac{1}{2} x^{\mathbf{T}}(t) G x(t) + \frac{1}{2} u^{\mathbf{T}} R u + \lambda^T (Ax(t) + Bu).$$

From the Hamiltonian, we have the optimality equation, derived from the term $u^{\mathbf{T}} R u$ with respect to u:

$$\frac{\partial}{\partial u}\left(u^{\mathbf{T}} R u\right) = \frac{\partial}{\partial u}\left(\sum_{i=1}^{n}\sum_{j=1}^{n} u_i R_{ij} u_j\right)$$

$$= \frac{\partial}{\partial u}\left(\sum_{i=1}^{n}\sum_{j=1}^{n} u_i \frac{1}{2}(R_{ij}u_j + R_{ji}u_i)\right)$$

$$= \frac{1}{2}\left(R + R^{\mathbf{T}}\right) u$$

$$= Ru$$

Derived from the term $\lambda^{\mathbf{T}}(Ax(t) + Bu)$, with respect to u:

$$\frac{\partial}{\partial u}\left(\lambda^{\mathbf{T}}(Ax(t) + Bu)\right) = \frac{\partial}{\partial u}\left(\lambda^{\mathbf{T}} B u\right)$$

$$= B^{\mathbf{T}}\lambda$$

Therefore, the partial derivative of H with respect to u is:

$$\frac{\partial H}{\partial u} = Ru + B^{\mathbf{T}}\lambda,$$

hence it follows that

$$u^* = -R^{-1} B^{\mathbf{T}} \lambda$$

we have that

$$\mathcal{H}(t,x,\lambda) = \overset{\min}{u \in \mathcal{X}} \left\{ \left\langle \lambda^{\mathbf{T}}, Ax + Bu \right\rangle + \frac{1}{2} \left[x^{\mathbf{T}} G x + u^{\mathbf{T}} R u \right] \right\},$$

using the *Hamilton-Jokobi-Bellman* optimality equation

$$\frac{\partial V}{\partial t} + \left\langle \frac{\partial V}{\partial x}, Ax \right\rangle - \frac{1}{2} \left\langle \frac{\partial V}{\partial x}, BR^{-1}B^{\mathbf{T}} \frac{\partial V}{\partial x} \right\rangle + \frac{1}{2} \left\langle x^{\mathbf{T}}, Gx \right\rangle = 0$$

We will now make the most important hypothesis-driven development, which allows us to determine V. Assuming that the value function for the linear quadratic problem has the form:

$$V(t,x) := \frac{1}{2} \left\langle x, P(t)x \right\rangle, \ (t,x) \in [0,T] \times \mathbb{R}^n,$$

assuming that $P : [0,T] \to \mathbb{R}^{n,n}$ is continuously differentiable, as the cost function is non-decreasing, and we can state that $P(t)$ is positive defined for all $t \in [0,T]$. The assumptions of symmetry for G, R are buried in the above calculations. Instead of using λ, wen found a matrix function P(t) such that $\lambda(t) = \frac{\partial V}{\partial x} = P(t)x(t)$.

Substituting the expression for V into the *HJB* equation, we obtained

$$\langle x, Y(t)x \rangle = 0,$$

in which

$$Y(t) = P'(t) + P(t)A + A^{\mathbf{T}}P(t) - P(t)BR^{-1}B^{\mathbf{T}}P(t) + G.$$

the problem now is to find a matrix function P such that $Y(t) \equiv 0$. The following theorem guarantees this result.

Theorem 7.3. *Let $P(t)$ be a continuous and differentiable symmetric matrix with respect to time t on an interval $[0,T]$, considering the Riccati equation:*

$$\frac{\partial P(t)}{\partial t} = -A^T P(t) - P(t)A + P(t)BR^{-1}B^T P(t) - G$$

in which A is a constant matrix of size $n \times n$; B is a constant matrix of size $n \times m$; R is a positive definite matrix of size $m \times m$; and G is a constant symmetric matrix of size $n \times n$. Optimal control is the form

$$u^* = -R^{-1}B^{\mathbf{T}}\lambda.$$

Then, for each initial condition $P(0) = P_0$, there is a unique solution $P(t)$ to the Riccati equation defined by $[0,T]$, associated with control systems (7.10) *to* (7.11).

Simple ODE techniques can be used to solve the problem because, once the Riccati matrix equation for P is solved, the control is given by an equation in x, and x is given by an ODE in u. The proof for this theorem can be seen in detail in Baumeister and Leitão (2008).

We considered the control system (7.10), whose governing matrix is

$$A = \begin{bmatrix} -\mu & 0 & 0 & 0 \\ 0 & -(\gamma+\mu+\eta) & 0 & 0 \\ 0 & (\eta-\epsilon) & -(\rho+\mu) & 0 \\ 0 & \gamma & \rho & -\mu \end{bmatrix}$$

The control operator is assumed to be

$$B = \begin{bmatrix} 1 & 0 \\ 0 & 1 \\ 0 & 0 \\ 0 & 0 \end{bmatrix},$$

and $$R = \begin{bmatrix} 2 & 0 \\ 0 & 2 \end{bmatrix}, \qquad G = \begin{bmatrix} 1 & 0 & 0 & 0 \\ 0 & 1 & 0 & 0 \\ 0 & 0 & 0 & 0 \\ 0 & 0 & 0 & 0 \end{bmatrix}.$$

The (7.10) system is added to a control measure to decrease COVID-19 transmission, in which the optimal control policy $u^* = -R^{-1}B^{\mathbf{T}}\lambda$ determines how the system should be controlled to minimize the cost functional. The main objective of optimal control is to reduce the number of individuals susceptible $S(t)$ to and infected $I(t)$ with COVID-19 in the population and the overall cost of controlling the disease dynamics. Then, the cost functional (7.11) can be rewritten as the following eq. (7.12)

$$J(u,x) = \frac{1}{2}\left[\int_0^T (S^2 + I^2 + u^2)dt\right], \tag{7.12}$$

with, $u^* = -[1/2\lambda \;\; 1/2\lambda]^{\mathbf{T}}$.

By solving the Riccati equation for internal control $u^*(t)$, we obtained eq. (7.13)

$$\frac{\partial P(t)}{\partial t} = -A^T P(t) - P(t)A + P(t)BR^{-1}B^T P(t) - G. \tag{7.13}$$

For this example, we specified the ingredients as follows: $T = 30$; $\mu = 0.02$; $\alpha = 0.2$; $\Delta = 0.2$; $\gamma = 0.1$; $\eta = 0.2$; $\epsilon = 0.1$; $\rho = 0.3$; $\lambda = 1.5$. And by using the fourth order Runge-Kutta method we solved the equation, as shown figure 3.

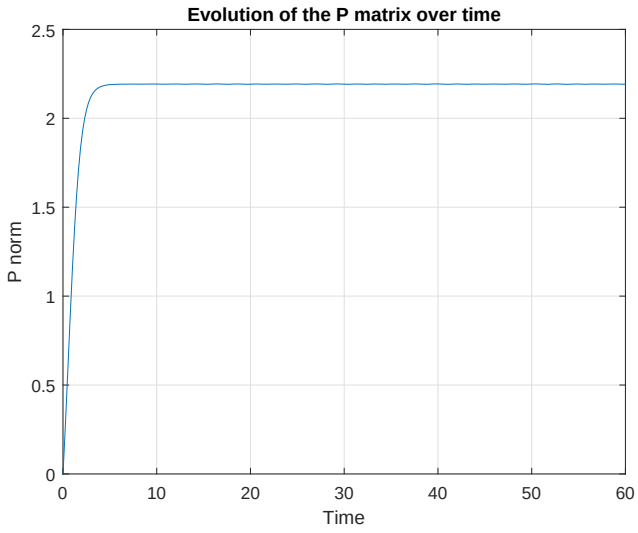

Figure 3: Evolution of the P norm.

The $P(t)$ matrix, obtained as the solution of the Riccati equation, is directly related to optimal control. This tool is used to find the control input that minimizes system costs over time. The $P(t)$ matrix norm in the context of the Riccati equation provides information about controlled system stability, indicating whether or not it has stabilized, as it converges to a constant value over time. The graph shows, according to figure 3, this evolution by indicating how optimal control also converges and ensures both stability and adequate performance for the entire controlled system. In the next section, we will show optimal control numerically.

8. Numerical simulations

We will see numerical simulations in this section to demonstrate the model dynamic characteristics, equilibrium point stability and optimal control.

Using MATLAB^{TM} software, we performed numerical simulation in model (2.3) and estimated the basic values of the model parameters. We will see the results of stabilization to endemic and disease-free equilibrium points. We showed how to solve the suggested optimal control problem. We simulated and compared different situations to control the spread of COVID-19. The results of simulation are shown in the following diagram.

In system (2.3), $\gamma = 0.1$, $\mu = 0.02$, $\rho = 0.3$, $\epsilon = 0.1$, $\eta = 0.2$, $\Delta = 0.2$, and $v = 0.05$. When $\alpha = 0.08$, we have $R_0 = 0.7143 < 1$, and with the initial condition $(9, 1, 0, 0)$, the solution converged to the free-disease solution $(2.8571, 0, 0, 0.0041)$. Figure 4 shows numerical simulation. From Theorem 5.2, we noticed that E_0 is globally asymptotically stable.

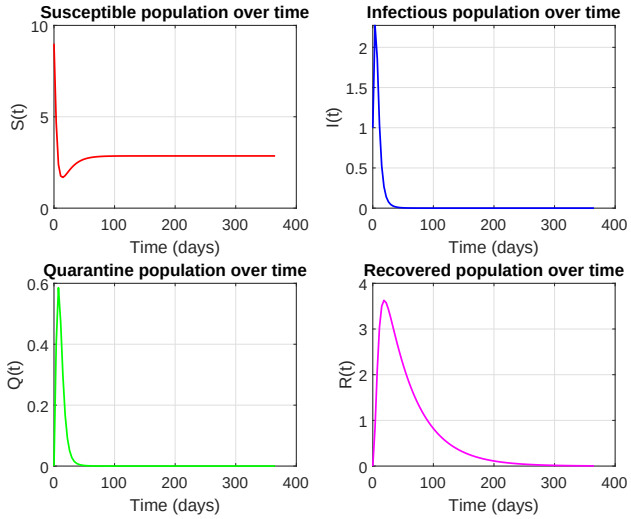

Figure 4: Variational curves of S, I, Q, and R

In system (2.3), $\gamma = 0.1$, $\mu = 0.02$, $\rho = 0.3$, $\epsilon = 0.1$, $\eta = 0.2$, $\Delta = 0.2$, and $v = 0.05$. When $\alpha = 0.2$, we have $R_0 = 1.7857 > 1$, and with the initial condition $(9, 1, 0, 0)$, the solution converges to the endemic disease solution $(1.6, 0.275, 0.0859, 2.6660)$. Figure 5 shows numerical simulation. From Theorem 5.4, we noticed that E^* is globally asymptotically stable.

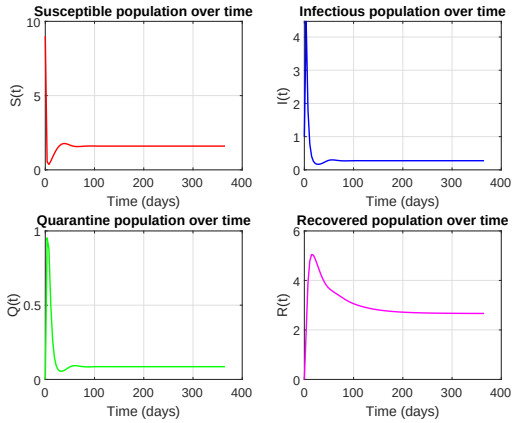

Figure 5: Variational curves of S, I, Q, and R

Additionally, we set the same initial conditions and parameters as in the previous simulation, and we had the following examples. The quarantine-free ($\eta = 0$) and vaccination-free ($v = 0$) model reproduction number R_0 is $16.6667 > 1$, as shown in numerical simulation figure 6. The reproduction number R_0 vaccination-free ($v = 0$) model is $R_0 = 6.2500 > 1$, as shown in numerical simulation in figure 7. The reproduction number R_0 quarantine-free ($\eta = 0$) model is $R_0 = 4.7619 > 1$, as shown in numerical simulation in figure 8.

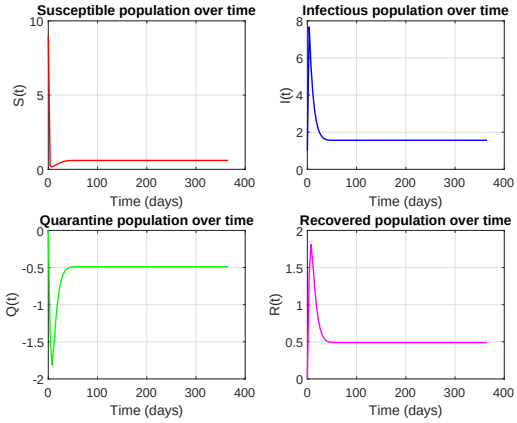

Figure 6: Variational curves of S, I, Q, and R with $R_0 = 16.6667 > 1$

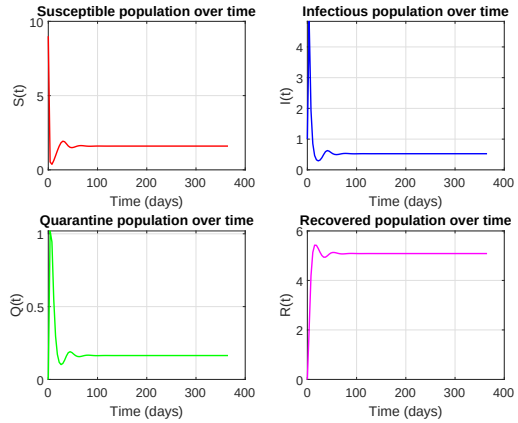

Figure 7: Variational curves of S, I, Q, and R with $R_0 = 6.2500$ and $v = 0$

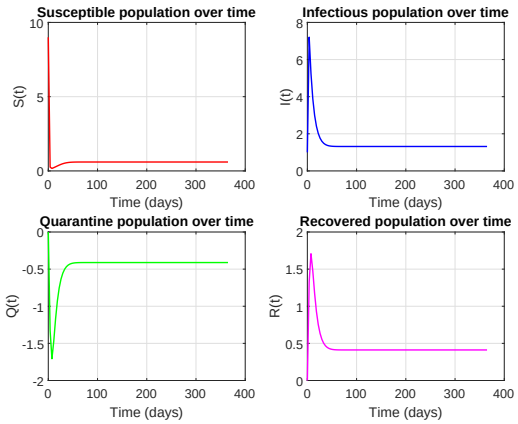

Figure 8: Variational curves of S, I, Q, and R with $R_0 = 4.7619$ and $\eta = 0$

Moreover, we have the evolution of the state variables without the presence of the optimal control strategy. Considering the Riccati equation (7.13), $T = 30$, $\gamma = 0.1$, $\mu = 0.02$, $\rho = 0.3$, $\epsilon = 0.1$, $\eta = 0.2$, $\Delta = 0.2$, and $v = 0.05$. When $\alpha = 0.2$, we have $R_0 = 1.7857 > 1$, and with the initial condition $(9, 1, 0, 0)$, figure 9 shows numerical simulation.

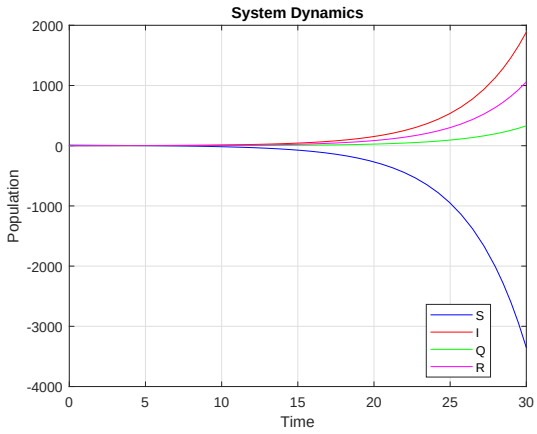

Figure 9: Variational curves of S, I, Q, and R without optimal control

In this next simulation, we will perform numerical simulations for an optimal control strategy given by theorem 7.3. Considering the Riccati equation (7.13), $T = 180$, $\gamma = 0.1$, $\mu = 0.02$, $\rho = 0.3$, $\epsilon = 0.1$, $\eta = 0.2$, $\Delta = 0.2$, and $v = 0.05$ and $\lambda = 0.5$. When $\alpha = 0.2$, we have $R_0 = 1.7857 > 1$, and with the initial condition $(9, 1, 0, 0)$, figure 10 shows numerical simulation.

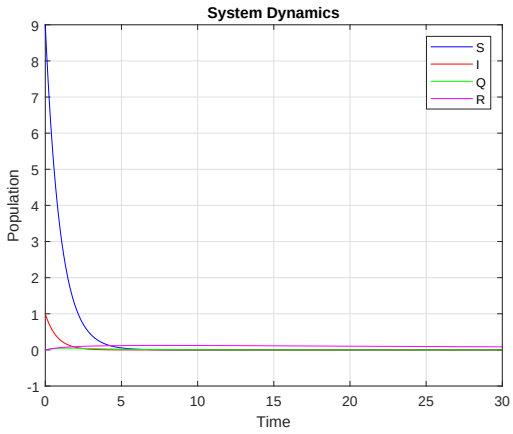

Figure 10: Variational curves of S, I, Q, and R with optimal control

9. Results

In this section, we will discuss and analyze the COVID-19 spread waves patterns presented in the numerical simulations previously. To do this analysis, we will take as a parameter the basic reproduction number R_0.

We have from Theorem 5.1 that if $R_0 < 1$, the solutions converge to disease-free equilibrium of system (2.3), as we can see in figure 4. This means that, when the number of newly infected $I(t)$ is zero in the system, the disease-free equilibrium point occurs. This can occur when the number of individuals susceptible to $S(t)$ is small as a result of vaccination or when the amount of infected $I(t)$ recovered $R(t)$ is small enough to prevent the disease from continuously spreading in the population. This confirms the fact that the system is also controllable (Theorem 6.3). Besides that, a system is controllable if, and only if it is stabilized (Micu and Zuazua (2004)).

On the other hand, when $R_0 > 1$, we have a system converging to endemic equilibrium solution of system $(1.6, 0.275, 0.0859, 2.6660)$, as in figure 5. In system (2.3), the endemic stabilization point occurs when the number of people entering the $I(t)$ compartment is equal to the number of people leaving the compartment for reasons of $Q(t)$ quarantine, $R(t)$ recovery, or death.

In other words, at endemic equilibrium point, the number of new cases is equal to the number of recovered or quarantined cases, thus providing a balance in the number of infected cases in the population over time. Actually,

$$\alpha SI = \mu I + \gamma I + \eta I = 0.088.$$

Note that R_0 depends as much on v as on η and $\dfrac{\partial R_0}{\partial v} > \dfrac{\partial R_0}{\partial \eta}$. In fact,

$$\frac{\partial R_0}{\partial v} = \frac{\Delta\alpha}{(\mu+v)^2(\gamma+\mu+\eta)}$$

and

$$\frac{\partial R_0}{\partial \eta} = \frac{\Delta\alpha}{(\mu+v)(\gamma+\mu+\eta)^2} \tag{9.14}$$

in which $\frac{\partial R_0}{\partial v} = 1.0449$ and $\frac{\partial R_0}{\partial \eta} = 0.0234$.

Continuing our analysis, we can see in the simulation presented in figure 7 that, when a system presents $v = 0$ and $\eta \neq 0$, the number of reproductions increases approximately 1.3 more than when considered $\eta = 0$ and v, with a 5% vaccination rate (simulation 8). We noticed that the number of basic reproduction increases very quickly when we consider $v = 0$ and $\eta = 0$ (simulation 6),

in which we do not consider any kind of control over the spread of the disease. From this, we concluded that the presence of the vaccine is more effective as a control strategy than just control of infectious individuals.

From the analysis, we noted that isolating infected individuals can be considered as a disease spread control strategy but as our main objective is to verify the effectiveness of the vaccine use strategy, we will take the isolation rate of constantly infected individuals equal to η and vary the population vaccination rate for optimal control simulations.

Finally we showed optimal control, taking into account 7.3, which provides us with an optimal control strategy $u^* = -R^{-1}B^{\mathbf{T}}\lambda$, minimizing the functional cost (7.11), which gives us the system performance over time. Considering $R_0 > 1$, we have here a context of spread of the disease, so we analyzed this scenario without the presence of an optimal control strategy (figure 9). We can see how state variables are unstable, and it is only possible to obtain a system stability by increasing the percentage of the vaccinated population, i.e., from 35% of the population immunized we can maintain spread curves stable. On the other hand, when we used the optimal control strategy u^*, it was possible to see a better system performance and consequently a reduction in coststhat we can obtain the same results with less effort in applying control (figure 10). Therefore, the vaccine presents itself as a state strategy to control system replenishment, effective in combating the spread of COVID-19.

10. Conclusion

In this article, we studied the behavior of COVID-19 spread by using a compartmental SIQR model, with vaccination as the main prevention strategy . We studied model equilibrium points and stability, controllability, and optimal control for the system, finally presenting some numerical simulations to support the theoretical results. From equilibrium points and stability analysis, we learned about two constant solutions: one was the disease disappearing quickly and the other continued to infect a small portion of the population, depending on the value of R_0. By using the simulations, we showed the behavior of system (2.3) and also learned that the presence of vaccination can decrease the basic reproductive number faster than the isolation of infectious individuals, eventually bringing the number of infections to endemic equilibrium. By applying optimal control strategies, it was possible to optimize the logistical costs of the

vaccine and reach endemic equilibrium more quickly.

We concluded this work by emphasizing that, for future work, this study can be carried out for the same models, combinations of varied control strategies, improving our knowledge about the behavior of this type of system and also our understanding of infectious diseases

References

Achaiah, N. C., Subbarajasetty, S. B., and Shetty, R. M. (2020). R_0 and R_e of COVID-19: Can we predict when the pandemic outbreak will be contained? *Indian J. Crit. Care Med.*, 24(11):1125–1127.

Baumeister, J. and Leitão, A. (2008). Introduction to theory of control and dynamic programming (in portuguese). In *Euclid's project*. IMPA, Rio de Janeiro.

Brauer, F., Castillo-Chavez, C., and Feng, Z. (2019). Simple compartmental models for disease transmission. In *Mathematical Models in Epidemiology*, pages 21–61. Springer New York.

Britton, T., Ball, F., and Trapman, P. (2020). A mathematical model reveals the influence of population heterogeneity on herd immunity to SARS-COV-2. *Science*, 396:846–849.

Kermark, M. and Mckendrick, A. (1927). Contributions to the mathematical theory of epidemics. *Proceedings of the Royal Society*, 115A:700–721.

Lisboa, S. A. and Rodrigues, L. R. S. (2023). Epidemiological model for building scenarios for the spread of COVID-19 in codó-MA. *Journal of Epidemiology and Infection Control (in Portuguese)*, 13(1):28–35.

Liu, Z., Magal, P., Seydi, O., and Webb, G. (2020). Understanding unreported cases in the covid-19 epidemic outbreak in wuhan, china, and the importance of major public health interventions. *Biology*, 9(3):50.

Lu, H., Ding, Y., Gong, S., and Wang, S. (2021). Mathematical modeling and dynamic analysis of siqr model with delay for pandemic covid-19. *Mathematical Biosciences and Engineering*, 18:3197–3214.

Ma, J. (2020). Estimating epidemic exponential growth rate and basic reproduction number. *Infectious Disease Modelling*, 5:129–141.

Ma, Y., Liu, J., and Li, H. (2018). Global dynamics of an siqr model with vaccination and elimination hybrid strategies. *Mathematics*, 6(12):328.

Micu, S. and Zuazua, E. (2004). An introduction to the controllability of partial differential equations. In *Quelques questions de théorie du contrôle, T. Sari ed.* Citeseer.

Odagaki, T. (2020). Exact properties of SIQR model for COVID-19. *Physica A*, 564:125564.